Acta Materia Medica

Research Article

Macrophage differentiation in enhancing hematopoietic function of ribonucleic acid for injection II via multi-omics analysis

Graphical abstract

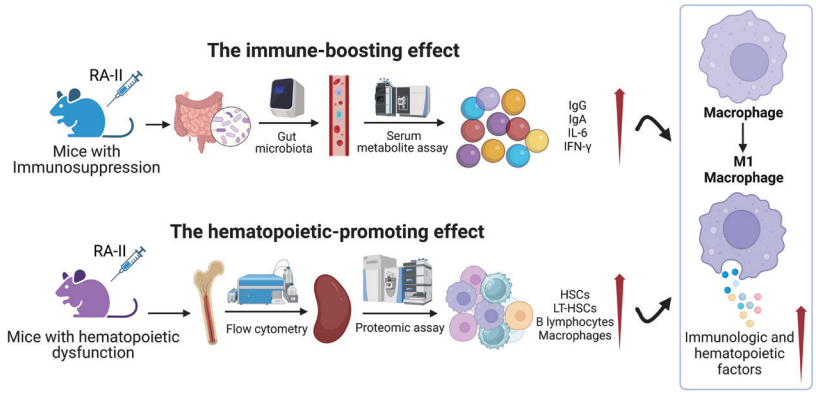

Highlights

- RA-II, a clinical adjuvant cancer therapy, utilizes immunotherapy to combat cancer.
- RA-II is rich in amino acids and nucleotides, which are essential for its biological potency.
- RA-II enhances the immune response and hematopoietic function.
- RA-II regulates the gut microbiota and serum metabolites.
- RA-II orchestrates macrophage differentiation towards the M1 phenotype.

Authors

Yuan Li, Meng Teng, Siyu Li, Hongxin Yang, Yuebo Zhang, Meihua Cui, Lanzhou Li and Di Wang

Correspondence

lilanzhou@jlau.edu.cn (L. Li);
jluwangdi@jlu.edu.cn (D. Wang)

In brief

RA-II is a clinical adjuvant therapy for cancer treatment based on immunotherapy. In this research, RA-II, rich in amino acids and nucleotides, has been confirmed to exhibit immune-boosting effects by influencing the gut microbiota and serum metabolites. Furthermore, it demonstrates hematopoietic-promoting effects by mediating macrophage M1 differentiation.

https://doi.org/10.15212/AMM-2024-0001
Acta Materia Medica 2024, Volume 3, Issue 3, p. 289-304

Acta Materia Medica

Research Article

Macrophage differentiation in enhancing hematopoietic function of ribonucleic acid for injection II via multi-omics analysis

Yuan Li[a,b], Meng Teng[a], Siyu Li[a], Hongxin Yang[a], Yuebo Zhang[c], Meihua Cui[c], Lanzhou Li[d,*] and Di Wang[a,d,e,*]

[a]School of Life Sciences, Jilin University, Changchun 130012, Jilin, China
[b]Cancer Research Center, School of Medicine, Xiamen University, Xiamen 361102, China
[c]Jilin Aodong Pharmaceutical Industry Group Yanji Co., Ltd., Yanji 133001, Jilin, China
[d]Engineering Research Center of Chinese Ministry of Education for Edible and Medicinal Fungi, College of Plant Protection, Jilin Agricultural University, Changchun 130118, Jilin, China
[e]Tianjin Institute of Industrial Biotechnology, Chinese Academy of Sciences, Tianjin 300308, China

***Correspondence:** lilanzhou@jlau.edu.cn (L. Li); jluwangdi@jlu.edu.cn (D. Wang)

Received: 2 January 2024; Revised: 29 April 2024; Accepted: 1 August 2024

Published online: 15 August 2024

DOI 10.15212/AMM-2024-0001

ABSTRACT

Ribonucleic acid for injection II is a clinical adjuvant cancer therapy treatment based on immunotherapy, which exerts its effects by enhancing immune function and suppressing tumor growth. However, the mechanism underlying the ameliorative effect on immunosuppressed hematopoietic dysfunction remains unclear. This study confirmed the immune-boosting and hematopoietic-promoting effects of ribonucleic acid for injection II, which has a wide distribution of molecular weights and is rich in amino acids and nucleotides. Ribonucleic acid for injection II influences the gut microbiota and serum metabolites to enhance immunity in immunosuppressed mice induced by CTX, while also mitigating bone marrow injury and increasing hematopoietic cells through mediating macrophage M1 differentiation, thereby improving hematopoietic dysfunction in mice.

Keywords: Ribonucleic acid for injection II, Immunity, Hematopoiesis, Macrophage Differentiation

1. INTRODUCTION

Macrophages are vital for the host innate immune system against pathogens and cancers, and also has a crucial regulatory role in immunity and hematopoiesis by balancing and coordinating different types of defense responses [1, 2]. Accordingly, classically activated macrophages (M1 phenotype) induced by pro-inflammatory signals, such as interferon (IFN)-γ plus lipopolysaccharide (LPS), express CD86 and secrete pro-inflammatory cytokines. In contrast, alternatively activated macrophages (M2 phenotype) are driven by anti-inflammatory cytokines and are associated with secretion of interleukin (IL)-10, transforming growth factor (TGF)-β, and arginase 1 (ARG1) [3, 4].

The tumor microenvironment can influence tumor-associated macrophages to adopt an immunosuppressive polarization, which inhibits the immune response and facilitates evasion from tumor-immune surveillance [5]. An imbalance in M1/M2 polarization results in an inefficient immune response, leading to immunosuppression. This imbalance can cause hematopoietic injury through cell-mediated cytotoxic mechanisms, resulting in multiple bone marrow failure syndromes that damage proliferating hematopoietic precursor cells [6]. The immune and inflammatory responses in the bone marrow largely affect hemopoietic stem cell (HSC) function [7]. Innate immune processes may synergistically act with inflammation to promote HSC self-renewal [8].

Immune cells, such as macrophages, are tightly regulated by the gut microbiota to maintain immune homeostasis [9]. Gut microbes regulate macrophage differentiation and modulate immune function by altering host serum metabolites [10]. Short-chain fatty acids and gram-negative bacterial LPS exert regulatory effects on inflammation by acting on macrophages [11]. *Pediococcus pentosaceus* CECT8330 reprograms macrophages from an M1 to an M2 phenotype, resulting in a decrease in IL-1β production and reduced reactive oxygen species (ROS) [12]. *Lacticaseibacillus casei* & *L. reuteri* inhibit toll-like receptor 4 (TLR4) to promote polarization of macrophages towards the M1 phenotype

[13]. The immune response impacts the emergence of HSCs, maintenance of hematopoietic homeostasis, and can cause or treat hematopoietic dysfunction in disease [14]. Activation of pro-inflammatory signaling cascades by macrophages with a pro-inflammatory phenotype may contribute to the formation of HSCs [15].

The main complications of radiotherapy and chemotherapy, such as immunosuppression, bone marrow suppression, and hematopoietic impairment, can cause delays or termination in cancer treatment [16, 17]. Macrophages can be polarized into M1 macrophages with immunotherapeutic efficiency during radiotherapy and chemotherapy, thereby modulating the tumor immune microenvironment from an immunosuppressive state to an immune-activated state [18]. The alkylating agent, cyclophosphamide (CTX), is widely used in tumor therapy but has toxic side effects, such as immunosuppression and myelosuppression. Therefore, CTX is commonly utilized to create mouse models with immunosuppression or hematopoietic injury induced by myelosuppression [19], which was successfully applied in our previous study [20]. Ribonucleic acid for injection II (RA-II) is a pure and bioactive ribonucleic acid (RNA) extracted from bovine pancreas that is approved in China to enhance immune function and inhibit tumors and reduce adverse reaction when combined with radiotherapy and chemotherapy (GYZZH22020007). RA-II suppresses tumor cell proliferation and induces programmed cell death, making RA-II a valuable therapeutic option for malignancies, such as pancreatic, liver, stomach, lung, and breast cancers, and soft tissue sarcoma [21]. Furthermore, RA-II has been utilized as an adjuvant in the management of hepatitis B [21]. However, the improvement effect of RA-II on immunosuppression-based hematopoietic injury and the underlying mechanism have not been investigated.

In the present study we conducted a compositional analysis of RA-II and demonstrated the protective effects in mice with immunosuppression and hematopoietic dysfunction. The hematopoietic ameliorating effect of RA-II may be associated with upregulation of immune- and hematopoiesis-related factors that are achieved by promoting macrophage polarization towards M1.

2. METHODS

2.1 Compositional analysis of RA-II

The RA-II molecular weight range, nucleotides (n = 5), hydrolyzed amino acids (n = 17), and total nitrogen content were examined. The RA-II molecular weight distribution was determined using a 1260 Infinity II MDS gel permeation chromatograph equipped with a PL aquagel-OH mixed-H column (8 μm, 7.5 mm × 300 mm; Agilent, Santa Clara, CA, USA). The column was isocratically eluted with a 1.0 mL/min flow rate using a 0.1 mol/L sodium nitrate solution. The RA-II hydrolyzed amino acid content was determined using a 1260 liquid chromatograph equipped with a C18 Shiseido column (5 μm, 4.6 mm × 250 mm; Agilent) [20]. The RA-II nucleotide content was determined using a 1200 liquid chromatograph equipped with a C_{18} column (5 μm, 4.6 mm × 250 mm; Agilent). The detection wavelength was 254 nm and the column was isocratically eluted with a flow rate of 1.0 mL/min using a mobile phase consisting of phosphate buffer and methanol (1000:40 ratio). The RA-II total nitrogen content was determined using a K9840 Kjeldahl nitrogen tester (Hanon Instruments, Jinan, Shangdong, China) [22].

2.2 Mice and cells

Seven-week-old male specific pathogen-free (SPF) BALB/c mice weighing 20 ± 2 g were obtained from Liaoning Changsheng Biotechnology Co. Ltd. (Shenyang, Liaoning, China). The mice had access to sterile water and food *ad libitum* and were housed under controlled conditions of temperature (22-24°C), humidity (40%-60%), and light (12-h light/dark cycle).

YAC-1 cells (TIB-160) were purchased from the American Type Culture Collection (ATCC, Rockefeller, MD, USA). The culture medium was RPMI-1640 medium (Gibco, CA, USA) supplemented with 10% fetal bovine serum and 1% penicillin-streptomycin. The culture environment was an incubator with 5% CO_2 and 95% air.

2.3 Immunosuppressed mouse model construction and drug administration

This study was approved by the Institution Animal Ethics Committee of Jilin University (No. SY202207013). Forty-five mice were acclimatized and fed for 1 week. Twenty-seven mice were randomly selected and injected intraperitoneally with 75 mg/kg of CTX (Sigma-Aldrich, St. Louis, MO, USA) for 3 days. The immunosuppressed mice were randomly divided into 3 groups (n = 9/group) as follows. An immunosuppressed group was injected intraperitoneally with 10 mL/kg of normal saline (NS). The RA-II-treated group received an intraperitoneal injection of RA-II (4.5 mg/kg; Jilin Aodong Pharmaceutical Group Co., Yanji, Jilin, China). The transfer factor capsule (TF)-treated group was administered 2.7 mg/kg of TF orally (Chengdu Lier Pharmaceutical Co., Chengdu, Sichuan, China) daily for 4 weeks. The remaining 18 mice were injected intraperitoneally with 10 mL/kg of NS for 3 d, then divided into 2 groups (n = 9/group). One group was injected intraperitoneally with 10 mL/kg of NS ($CTRL_I$ group). The other group was treated with RA-II at a dose of 4.5 mg/kg for 4 weeks. The body weights were recorded regularly.

The mice were euthanized 2 h after the last treatment. Blood, heart, liver, spleen, lung, kidney, and thymus samples were collected. The feces were collected from the cecum in a sterile environment. The collected samples were stored at –80°C for subsequent analysis.

Splenocytes were harvested for analysis of natural killer (NK) cell activity and T lymphocyte proliferative capacity [20]. Briefly, splenocytes (1×10^6 cells/well) were

mixed with YAC-1 cells (1 × 10^5 cells/well) in 96-well plates and incubated at 37°C for 4 h. The cytotoxic activity of the NK cells was measured using an LDH cytotoxicity assay kit (C0016; Beyotime, Shanghai, China) in accordance with the manufacturer's instructions.

Splenocytes (1 × 10^6 cells/well) were cultured in 96-well plates and treated with concanavalin A (ConA; Shanghai yuanye Bio-Technology Co., Shanghai, China). The control group was not treated with ConA. The 96-well plates were incubated at 37°C for a duration of 48 h. The thiazolyl blue tetrazolium bromide assay (MTT; Sigma-Aldrich, St. Louis, MO, USA) was performed to detect splenocyte proliferation.

2.4 Establishment of a mouse model with hematopoietic dysfunction and drug administration

This study was approved by the Institution Animal Ethics Committee of Jilin University (No. SY202207014). Fifty mice were acclimatized and fed for 1 week. Thirty mice were randomly chosen and injected intraperitoneally with 100 mg/kg of CTX for 3 d to establish a hematopoietic dysfunction mouse model. The mice were then randomly divided into 3 groups (n = 10/group). A group with hematopoietic dysfunction was intraperitoneally injected with 10 mL/kg of NS, a group treated with RA-II received an intraperitoneal injection of 4.5 mg/kg of RA-II, and a group treated with recombinant human granulocyte colony-stimulating factor (rhG-CSF) was intraperitoneally injected with 22.5 μg/kg of rhG-CSF (Shandong Qilu Pharmaceutical Co., Jinan, Shandong, China) daily for 6 weeks. The remaining 20 mice were intraperitoneally injected with 10 mL/kg of NS for 3 d, then divided into 2 groups (n = 10/group). One group was intraperitoneally injected with 10 mL/kg of NS ($CTRL_H$ group), while the other group received an injection of 4.5 mg/kg of RA-II with treatment for a duration of 6 weeks. Body weights were recorded regularly.

Animals were euthanized 2 h following the last treatment. Heart, liver, spleen, kidney, lung, and femur samples were collected. The collected samples were stored at –80°C for subsequent analysis.

Bone marrow cells were extracted from the femurs in a sterile environment. Erythrocytes were removed from the cells mentioned above according to the manufacturer's instructions for red blood cell (RBC) lysis buffer (00-4300-54; Gibco). The concentration of cells was adjusted to 10^6 cells/100 μL using staining buffer, then staining was performed. The number of HSCs ($Lin^-Sca\text{-}1^+c\text{-}Kit^+$), long-term (LT)-HSCs ($Lin^-Sca\text{-}1^+c\text{-}Kit^+CD48^-CD150^+$), B lymphocytes ($CD45^+CD19^+$), and macrophages ($CD11b^+F4/80^+$) in samples of bone marrow-derived mononuclear cells from mice with hematopoietic dysfunction was detected using flow cytometry. The experimental protocols were performed in accordance with the manufacturer's instructions, as previously described [23]. The information on the antibodies used is listed in **Table 1s**.

2.5 Immunosuppressed mice gut microbiota assay

Total genomic DNA was extracted from cecum contents (n = 4/group) collected from $CTRL_I$, and vehicle- and RA-II-treated immunosuppressed mice following the manufacturer's instructions for the Omega Soil DNA kit (M5635-02; Omega Bio-Tek, Norcross, GA, USA). The nearly full-length bacterial 16S rRNA genes were amplified by PCR amplification [24]. The bacterial sequences have been deposited in the NCBI Sequence Read Archive under the accession number, PRJNA1008547 (https://www.ncbi.nlm.nih.gov/sra/PRJNA1008547).

2.6 Immunosuppressed mice serum metabolite assay

The metabolites in sera (n = 4/group) collected from $CTRL_I$, and vehicle- and RA-II-treated immunosuppressed mice were analyzed using ultra-high-performance liquid chromatography (UHPLC; Vanquish, Thermo Fisher, Germering, Bayern, Germany) equipped with an Acquity UPLC BEH Amide chromatography column (1.7 μm, 2.1 mm × 100 mm; Waters, Milford, MA, USA). The analysis was performed on a Q-Exactive Orbitrap mass spectrometry (MS; Thermo Fisher, Bremen, Germany). The sera were analyzed for significant changes in differential metabolites and these metabolites were then subjected to cluster and correlation analyses, as performed in our previous study [24].

2.7 Proteomic assay of spleens collected from hematopoietic dysfunction mice

Label-free quantification (LFQ) of protein levels was performed on spleen tissues collected from $CTRL_H$, and vehicle- and RA-II-treated mice with hematopoietic dysfunction. Cleaved proteins were quantified using the BCA assay and precipitated with acetone. The proteins were resuspended for tryptic digestion to remove SDC, desalted, then separated and analyzed by a nano-UPLC (EASY-nLC1200; Thermo Fisher, Waltham, MA, USA) coupled with Q-Exactive MS (Finnigan; Thermo Fisher, Bremen, Germany). The differential proteins were further analyzed, as in our previous study [24].

2.8 Hematoxylin and eosin staining assay

The femurs collected from mice in **Experiment 2.4** were fixed in a 4% paraformaldehyde solution (BL539A; Biosharp, Guangzhou, Guangdong, China) for 48 h and decalcified using an EDTA decalcification solution. The organs, including the heart, liver, spleen, lung, kidney, and thymus collected from **Experiments 2.3 and 2.4** were fixed in 4% paraformaldehyde for 48 h. The organs were embedded in paraffin along with the decalcified femurs. Then, the organs were cut into 5-μm sections and stained with hematoxylin and eosin, as described in previous studies [20, 23]. A pathologic evaluation and analysis were performed using a microscope.

2.9 Immunohistochemical staining assay

The paraffin sections of spleens collected from mice in **Experiment 2.3** and the femurs collected from mice in **Experiment 2.4** were deparaffinized for antigen retrieval, blocked with a 3% hydrogen peroxide solution, and sealed with 3% bovine serum albumin. The sections were incubated overnight at 4°C with the primary antibody, followed by a 50-min incubation at 20°C with the secondary antibody. After staining with 3,3′-diaminobenzidine, the nuclei were re-stained with hematoxylin. The slices were dehydrated, sealed with neutral gum, and observed under a microscope [25]. The antibody details are listed in **Table 2s**.

2.10 Immunofluorescence analysis

Bone marrow paraffin sections of $CTRL_H$, and vehicle- and RA-II-treated mice with hematopoietic disfunction were deparaffinized for antigen retrieval, blocked with a 3% hydrogen peroxide solution, and incubated with serum. Sections were incubated with primary antibodies against CD86, CD206, reticulon 1 (RTN1), magnesium transporter 1 (MAGT1), and galectin-3 (Gal-3) at 4°C overnight, followed by incubation with a secondary antibody for 50 min at 20°C. The nuclei were re-stained with 4′,6-diamidino-2-phenylindole after incubation with tyramide signal amplification for 20 min at 20°C. The sections were sealed by adding anti-fluorescence quenching sealer and observed under a microscope [25]. The antibody details are listed in **Table 3s**.

2.11 Western blot

The spleen tissues collected from mice in **Experiments 2.3 and 2.4**, and bone marrow collected from mice in **Experiment 2.4** were mixed with radio immunoprecipitation assay (RIPA) lysate (20-188; Millipore, Billerica, MA, USA) containing a protease and phosphatase inhibitor cocktail (P002; NCM Biotech, Suzhou, Jiangsu, China). The spleen tissues were ground in a high-throughput tissue mill and centrifuged at 16,000 g for 5 min. The supernatant was extracted and centrifuged again under the same conditions. The resulting supernatant from the final separation was collected as the lysate. The protein concentration of the collected lysate was measured according to the BCA kit instructions (Thermo Fisher, Waltham, MA, USA) and 40 μg of total proteins per group were separated by 7.5%-12.5% sodium dodecyl sulfate polyacrylamide gel electrophoresis (SDS-PAGE). The gel separated by electrophoresis was transferred onto polyvinylidene difluoride membranes. A rapid closure solution (GF1815; GeneFirst, Shanghai, China) was applied to seal the membranes. The membranes were incubated with the corresponding primary and secondary antibodies. Target imprints were detected using a highly sensitive chemiluminescence detection kit (GK10008; GlpBio, Montclair, CA, USA) and a gel imager (Tanon 5200; Tanon Science & Technology, Shanghai, China) [20, 23]. ImageJ (v1.8.0; National Institutes of Health, Bethesda, MD, USA) was utilized for quantitative analysis. The antibody details are listed in **Table 4s**.

2.12 Enzyme linked immunosorbent assay (ELISA)

Spleens collected from mice in **Experiment 2.3** were crushed using a high-throughput tissue grinder. After centrifugation at 16,000 g for 5 min, the supernatant was collected. The protein content of spleen homogenates was determined using a BCA kit (A53225; Thermo Fisher, Waltham, MA, USA). The immunoglobulin (Ig) G, IgA, IL-6, and IFN-γ levels were measured using ELISA, according to the manufacturer's instructions [20]. The ELISA kit details are presented in **Table 5s**.

2.13 Statistical analysis

One-way ANOVA based on Tukey's *post-hoc* test was performed using BONC DSS Statistics (v25.0; IBM Corporation, Armonk, NY, USA) to determine statistical significance. Results were considered statistically significant at a P value <0.05 and are presented as the mean ± standard error of the mean.

3. RESULTS

3.1 RA-II compositional analysis

The molecular weight distribution of RA-II is 500-1000 kDa (0.24%), 300-500 kDa (3.39%), 200-300 kDa (9.08%), 100-200 kDa (27.44%), 50-100 kDa (23.44%), 30-50 kDa (35.04%), and 29.578-30 kDa (1.37%; **Table 1**). Seventeen amino acids, including proline (22435.95 mg/kg), glycine (1196.94 mg/kg), and threonine (91.78 mg/kg), were detected. RA-II contained 5 nucleotides with concentrations of cytosine (2.73 mg/kg), uracil (10.79 mg/kg), guanine (18.94 mg/kg), adenine (14.39 mg/kg), and hypoxanthine (3.31 mg/kg; **Table 1**). The total nitrogen content of RA-II was 2.75 g/100 g (**Table 1**).

3.2 RA-II improves immunity by regulating macrophage M1 differentiation

3.2.1 RA-II boosts immunity in immunosuppressed mice. The spleens of immunosuppressed mice exhibited large extramedullary hematopoietic foci infiltrated with multinucleated giant cells, which were reversed by RA-II administration (**Figure 1A**). No obvious pathologic changes were observed in the heart, liver, lung, kidney, or thymus of the experimental mice (**Figure S1**). Low body weight ($P < 0.001$; **Table 6s**), the thymus index ($P < 0.05$; **Table 6s**), NK cell cytotoxic activity ($P < 0.001$; **Figure 1B**), and T lymphocyte proliferation ($P < 0.001$; **Figure 1C**) were characteristics of immunosuppressed mice. RA-II alleviated the decrease in body weight ($P < 0.05$; **Table 6s**), NK cell cytotoxic activity (81.0%, $P < 0.01$; **Figure 1B**), and T lymphocyte proliferation (21%, $P < 0.001$; **Figure 1C**) as well as a reduction in the thymus index among immunosuppressed mice (**Table 6s**). RA-II administration increased the IgG, IgA, IL-6, and IFN-γ levels in spleen tissues by 28.8% ($P < 0.01$), 31.6%

Table 1 | Molecular weight distribution, amino acid content, nucleotide content, and total nitrogen content of RA-II.

Items detected	Result
Molecular weight distribution	
MW (kDa)	Percent MW%
500-1000	0.24
300-500	3.39
200-300	9.08
100-200	27.44
50-100	23.44
30-50	35.04
29.578-30	1.37
Amino acid content	
Name	mg/kg
Aspartic	439.77
Glutamic	397.71
Serine	175.91
Glycine	1196.94
Arginine	42.07
Threonine	91.78
Alanine	26.77
Proline	22435.95
Isoleucine	122.37
Lysine	217.97
Histidine	<1.70
Tyrosine	<2.57
Valine	<1.70
Methionine	<2.45
Cystine	<21.80
Leucine	<2.43
Phenylalanine	<2.96
Nucleotide content	
Name	mg/kg
Cytosine nucleotide	2.73
Uracil nucleotide	10.79
Guanine nucleotide	18.94
Adenine nucleotide	14.39
Hypoxanthine nucleotide	3.31
Total nitrogen content	
Name	g/100 g
N	2.75

RA-II, ribonucleic acid for injection II.

($P < 0.01$), 46.7% ($P < 0.001$), and 42.3% ($P < 0.001$) in immunosuppressed mice (Figure 1D-G). These findings indicate that RA-II has immunomodulatory activity.

3.2.2 RA-II affects gut microbiota and serum metabolites in immunosuppressed mice. Among the $CTRL_I$, vehicle-treated, and RA-II-treated immunosuppressed mice, there were 299 shared operational taxonomic units (OTUs). The number of unique OTUs in the 3 groups was 1103, 808, and 488, respectively (Figure 2A). An altered microbial community structure was observed in RA-II-treated immunosuppressed mice, as indicated by the principal coordinate analysis plot beta diversity based on Jaccard's distance algorithm (Figure 2B). The top 25 bacteria in the 3 groups with the greatest variation in abundance were analyzed using random forest analysis to assess the importance of different species and rank the bacteria according to importance at the genus level (Figure 2C and Table 7s). The abundance of bacteria, such as *Ruminococcus*, was decreased in CTX-treated mice compared to normal mice, but this decrease was reversed after administration of RA-II (Figure 2C).

Furthermore, metabolites in the serum of immunosuppressed mice were analyzed using UHPLC-Q-Exactive Orbitrap MS. Metabolites consistent with the trend of metabolite changes in $CTRL_I$ and RA-II-treated immunosuppressed mice were selected for further analysis (Table 8s). RA-II decreased the levels of 14 metabolites and increased the levels of 5 metabolites compared to immunosuppressed mice (Figure 2D, Table 8s). A positive correlation existed between the 12(S)-HETE and L-carnitine levels, as well as between the solasodine and uridine levels. However, there was a negative correlation between 12(S)-HETE and uridine, as well as between L-carnitine and uridine (Figure 2E). There was a positive correlation between the uridine level and the abundance of *Ruminococcus* according to correlation analysis between differential bacteria and altered metabolites (Figure 2F). These results suggest that RA-II may modify the gut microbiota composition, thereby potentially impacting serum metabolites and immunity.

3.2.3 Macrophage M1 polarization is involved in RA-II-mediated immunity enhancement. Among the metabolites influenced by RA-II, the roles of A-769662 [26], 12(S)-HETE [27], palmitic acid [28], solasodine [29], uridine [30], and L-carnitine[31] were shown to be associated with macrophages (Figure 2D, Table 8s). The relationship between macrophage regulation of RA-II and enhancement of immunity was further explored. As shown in Figure 3A, the levels of M1 macrophage-associated proteins (CD86, inducible nitric oxide synthase [iNOS], monocyte chemotactic protein [MCP]-1, IL-21, IL-2, IL-12B, and cyclooxygenase [COX2]) were upregulated by 107.5% ($P < 0.05$), 72.6% ($P < 0.05$), 131.9% ($P < 0.01$), 195.4% ($P < 0.01$), 294.1% ($P < 0.05$), 188.3% ($P < 0.05$), and 52.2% ($P < 0.05$), respectively, in the spleens of immunosuppressed mice after RA-II

Acta Materia Medica

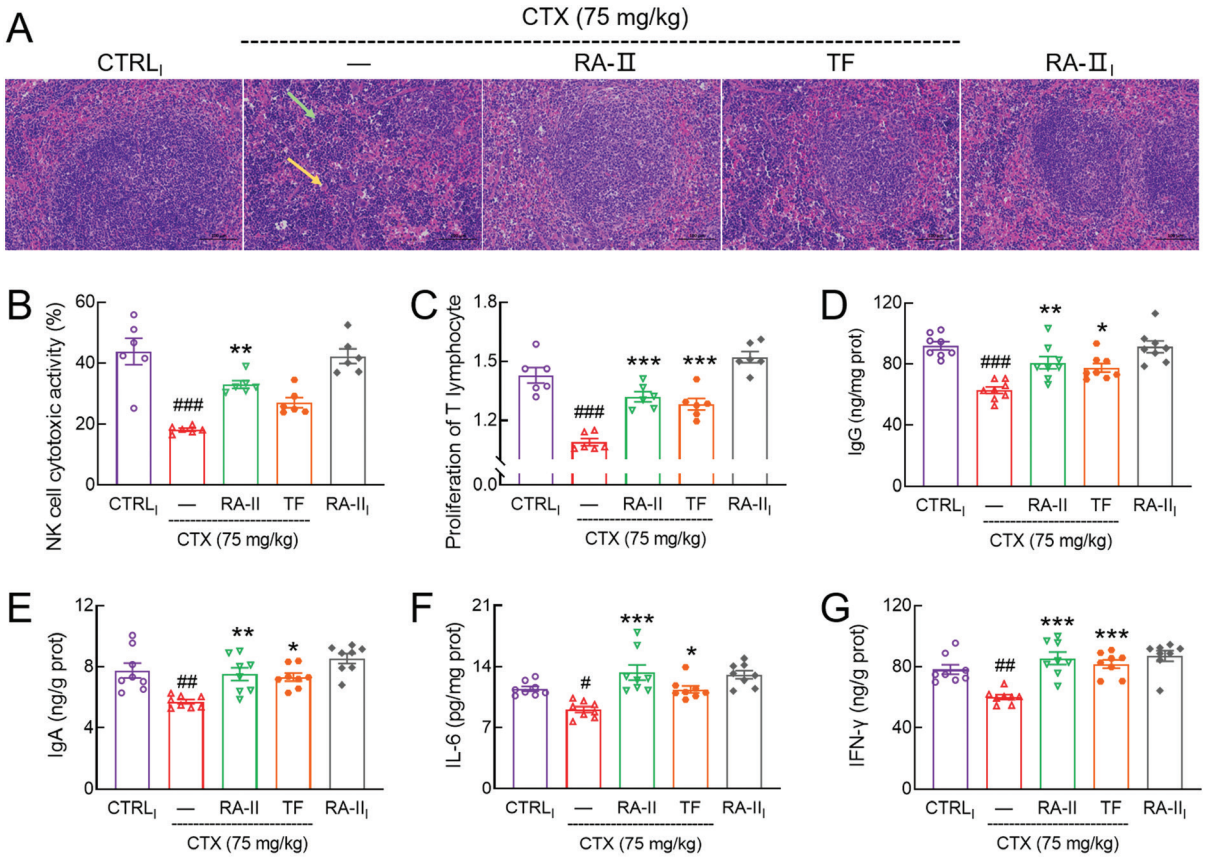

Figure 1 | RA-II boosts immunity in immunosuppressed mice.
(A) RA-II restored the histomorphology in spleens (200 ×, scale bar: 100 μm). The green arrow indicates the presence of extramedullary hematopoietic foci, while the yellow arrow points to multinucleated giant cells. RA-II enhanced the (B) NK cell cytotoxic activity and (C) T lymphocyte proliferation (n = 6/group). The effects of RA-II on cytokines, including (D) IgG, (E) IgA, (F) IL-6, and (G) IFN-γ, in spleens (n = 8/group). Data are presented as the mean ± SEM. $^{\#}P < 0.05$, $^{\#\#}P < 0.01$, and $^{\#\#\#}P < 0.001$ *vs.* CTRL$_|$; $^{*}P < 0.05$, $^{**}P < 0.01$, and $^{***}P < 0.001$ *vs.* vehicle-treated immunosuppressed mice.

administration. RA-II increased iNOS levels by 157.8% ($P < 0.001$) and decreased ARG1 levels by 59.1% ($P < 0.01$) in the spleens of immunosuppressed mice (Figure 3B), as shown by immunohistochemical staining. Additionally, the viability of macrophages in RAW 264.7 cells was not significantly affected by RA-II treatment at 0.05 or 0.1 mg/mL compared to the control group (Figure S4A). The administration of 0.05 and 0.1 mg/mL of RA-II significantly enhanced the expression levels of CD86, iNOS, IL-12B, and IL-21 expression in RAW 264.7 cells ($P < 0.05$; Figure S4B and S4C). These results suggest that M1 macrophages are involved in RA-II-enhanced immunity.

3.3 RA-II improves hematopoietic dysfunction in mice by mediating M1 differentiation

3.3.1 RA-II alleviates bone marrow injury and increases hematopoietic cells in mice with hematopoietic dysfunction. RA-II alleviated CTX-induced weight loss (Table 9s), as well as the severe abnormal bone tissue architecture, massive cytopenia, and fatty degeneration in the bone marrow cavity, and extensive loss of bone trabeculae (Figure 4A) in mice with hematopoietic dysfunction. Administration of RA-II resolved the abnormal spleen pathologic changes in mice with hemopoietic dysfunction, which was characterized by structural disorganization of splenic nodules, decreased lymphocyte count, increased interstitial space in some areas, and necrosis of cells with fragmented nuclei and an increased number of multinucleated macrophages (Figure S2). No significant effects of RA-II on the heart, liver, lung, or kidney were noted (Figure S2). RA-II significantly alleviated the loss of HSCs ($Lin^-Sca\text{-}1^+c\text{-}Kit^+$), LT-HSCs ($Lin^-Sca\text{-}1^+c\text{-}Kit^+CD48^-CD150^+$), B lymphocytes ($CD45^+CD19^+$), and macrophages ($CD11b^+F4/80^+$) by 134.5% ($P < 0.01$), 72.5% ($P < 0.05$), 147.0% ($P < 0.05$), and 53.7% ($P < 0.01$; Figure 4B) respectively, in the bone marrow of mice with hematopoietic dysfunction. RA-II enhanced hematopoiesis in mice by promoting the levels of hematopoietic cells in the bone marrow.

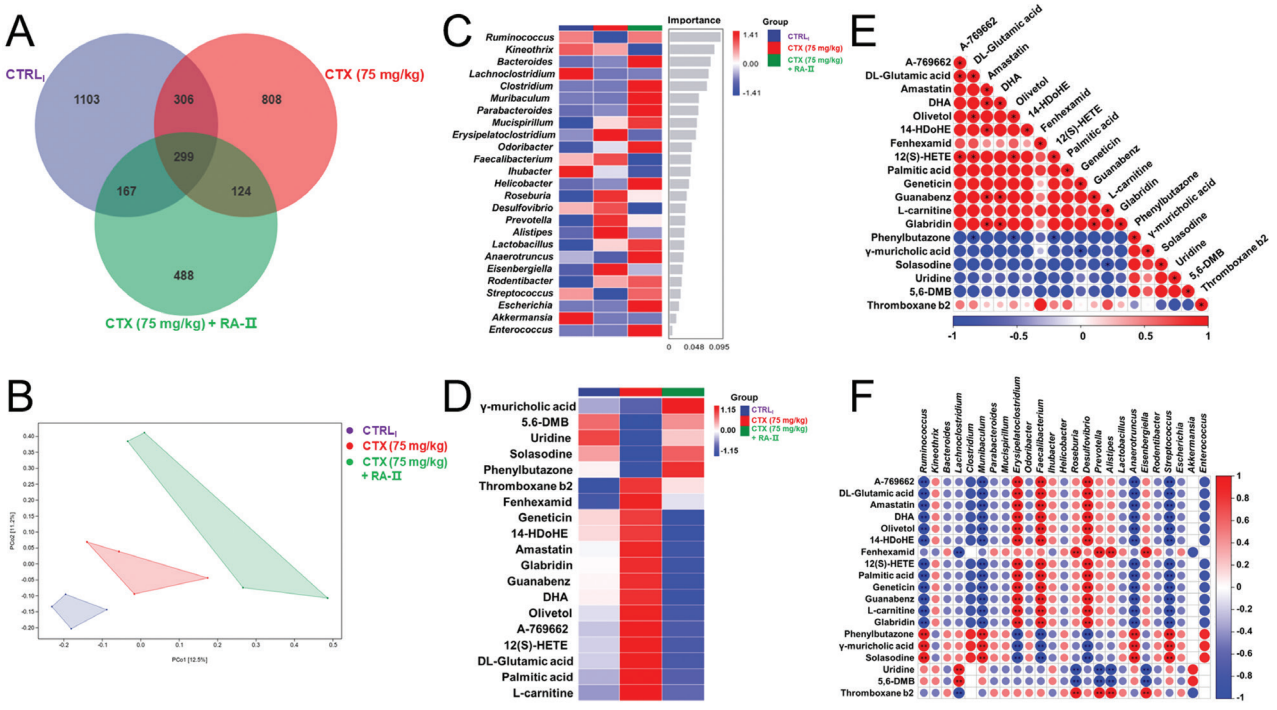

Figure 2 | RA-II modulated gut microbiota and serum metabolites in immunosuppressed mice.
The alteration of gut microbiota in the cecum feces and serum metabolites was analyzed by 16S rRNA sequencing and UHPLC-Q-Exactive Orbitrap MS, respectively (n = 4/group). (A) Venn diagram. (B) Principal coordinate analysis of unweighted UniFrac distance derived from beta diversity analysis. (C) Random forests at the genus level with heat maps to display marker species indicating the top 25 differences in importance. (D) Heatmap displaying 19 significantly altered serum metabolites. (E) Correlation analysis of the differential metabolites. (F) Correlation analysis between differential metabolites and the gut microbiota.

3.3.2 RA-II regulates macrophages based on proteomic analysis of spleens in mice with hematopoietic dysfunction. Forty-one significantly altered proteins were selected for further evaluation in the spleens of mice with hematopoietic dysfunction, based on label-free quantification. RA-II up- and down-regulated 24 and 17 types of proteins, respectively (Figure 5A, Table 10s). Among 41 proteins, RTN1, MAGT1, and Lgals3bp expression was significantly increased by RA-II administration (Figure 5A). Analysis of differentially expressed proteins using the search tool for recurring instances of neighboring genes (STRING) database revealed the interactions (Figure 5B). RA-II significantly increased RTN1, MAGT1, Gal-3, CD86, IL-1β, IL-6, and C-X-C motif chemokine ligand (CXCL) 1 expression by 76.8% ($P < 0.01$), 121.2% ($P < 0.001$), 114.9% ($P < 0.001$), 774.0% ($P < 0.001$), 650.6% ($P < 0.01$), 214.2% ($P < 0.05$), and 119.0% ($P < 0.001$), respectively. CD206 expression was decreased in the spleens of mice with hematopoietic dysfunction by 56.8% ($P < 0.001$; Figure 5C). Additionally, the RTN1, MAGT1, and Gal-3 levels in the bone marrow of mice with hematopoietic dysfunction were upregulated by 771.4% ($P < 0.05$), 697.8% ($P < 0.01$), and 285.0% ($P < 0.05$), respectively, after RA-II administration (Figure 5D). Proteins regulated by RA-II were expressed in the immune system, spleen, hematopoietic system, bone marrow-derived macrophages, and macrophages (Figure S3A). These proteins had mammalian phenotype ontologs (MPOs) associated with immune and hematopoietic system phenotypes (Figure S3B). The proteins significantly influenced by RA-II were mainly enriched in Wiki pathways associated with macrophage markers, the IL-6 signaling pathway, EPO receptor signaling, and type II interferon signaling (IFNG; Figure S3C). These proteins are involved in biological processes, such as regulation of the immune system, hemopoiesis, and myeloid cell differentiation (Figure S3D), according to gene ontology (GO) enrichment analysis. RA-II may enhance hematopoietic function through promoting macrophage differentiation.

3.3.3 RA-II promotes the differentiation of macrophages into the M1 phenotype. F4/80 and CD11b are the main markers for identifying macrophages [32]. The positive regions of F4/80 and CD11b in the bone marrow of mice with hematopoietic dysfunction were elevated by 392.3% ($P < 0.001$) and 352.2% ($P < 0.001$), respectively, after RA-II administration (Figure 6A). This finding is consistent with the above results from flow cytometry, confirming that RA-II increased the content of macrophages in the bone

Acta Materia Medica

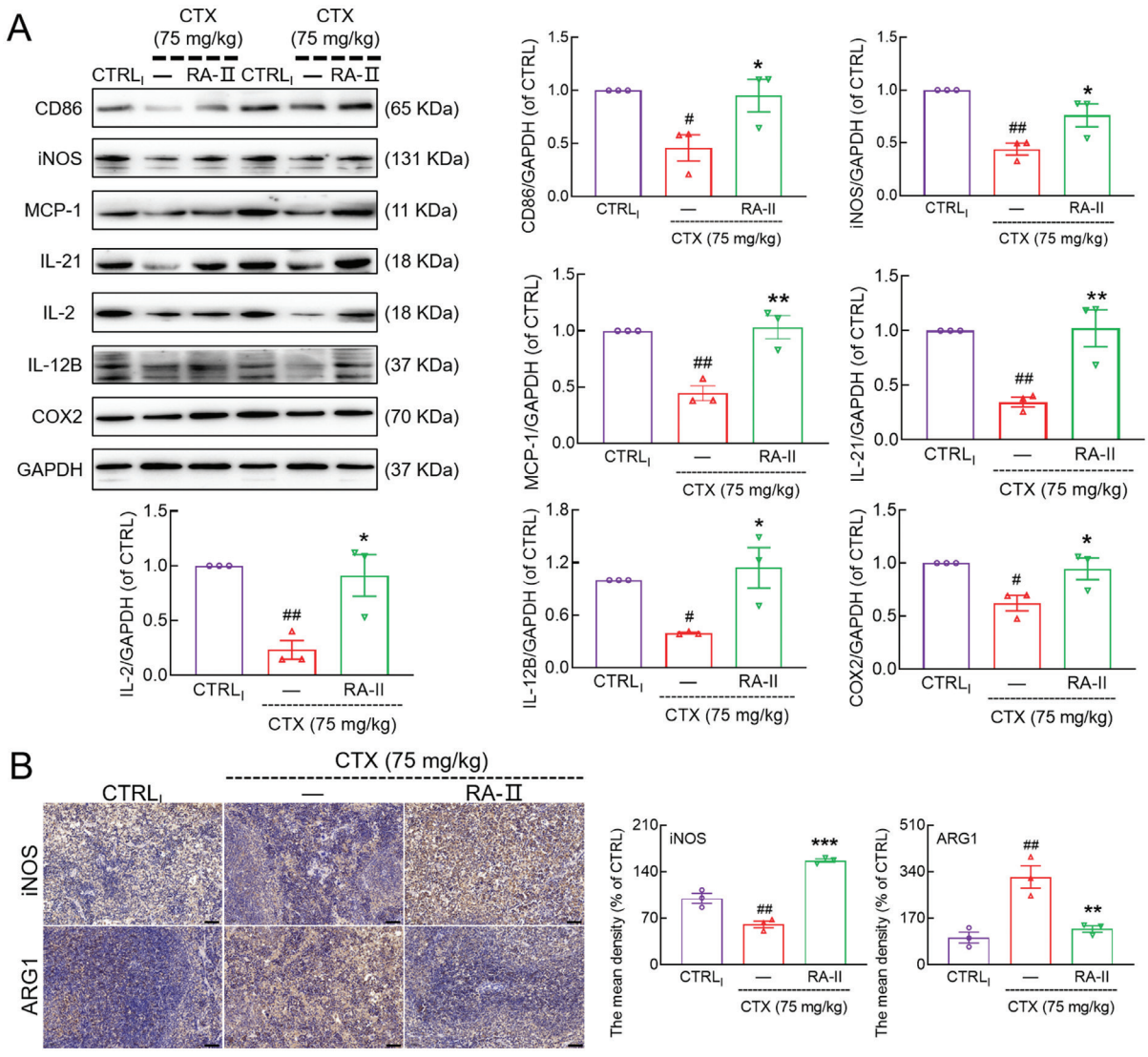

Figure 3 | RA-II influences the levels of proteins and cytokines related to immune function in immunosuppressed mice.
(A) RA-II enhanced the expression of CD86, iNOS, MCP-1, IL-21, IL-2, IL-12B, and COX2 in the spleens detected via western blot. (B) RA-II enhanced the iNOS level and suppressed the ARG1 level in the spleens detected by immunohistochemical staining (400 ×, scale bar: 50 μm). Data are presented as the mean ± SEM (n = 3/group). $^{\#}P < 0.05$ and $^{\#\#}P < 0.01$ *vs.* $CTRL_I$; $^{*}P < 0.05$, $^{**}P < 0.01$ and $^{***}P < 0.001$ *vs.* vehicle-treated immunosuppressed mice.

marrow. RA-II administration increased CD86 expression ($P < 0.001$) and decreased CD206 expression ($P < 0.01$) in the bone marrow of mice with hematopoietic dysfunction (Figure 6B), suggesting a RA-II-promoting effect on macrophage M1 differentiation.

Stimulating M1 macrophages leads to elevated IL-1β, IL-6, and CXCL1 levels [33]. RA-II administration increased CD86 and IL-1β expression by 434.1% ($P < 0.05$) and 125.1% ($P < 0.01$), respectively, while decreasing CD206 expression by 85.7% ($P < 0.05$) in the bone marrow of mice with hematopoietic dysfunction (Figure 6C). Immunohistochemical staining further confirmed the enhanced impact of RA-II on the expression of IL-1β, IL-6, and CXCL1 within the bone marrow (Figure 6D). Additionally, administration of 0.05 and 0.1 mg/mL of RA-II significantly enhanced the levels of IL-1β, IL-6, and CXCL1 expression in RAW 264.7 cells ($P < 0.01$; Figure S4B and S4C). RA-II promoted differentiation of macrophages toward the M1 phenotype and secretion of related proteins in the bone marrow of mice with hematopoietic dysfunction.

4. DISCUSSION

The present data confirmed that RA-II elevates the immune and related hematopoietic function via

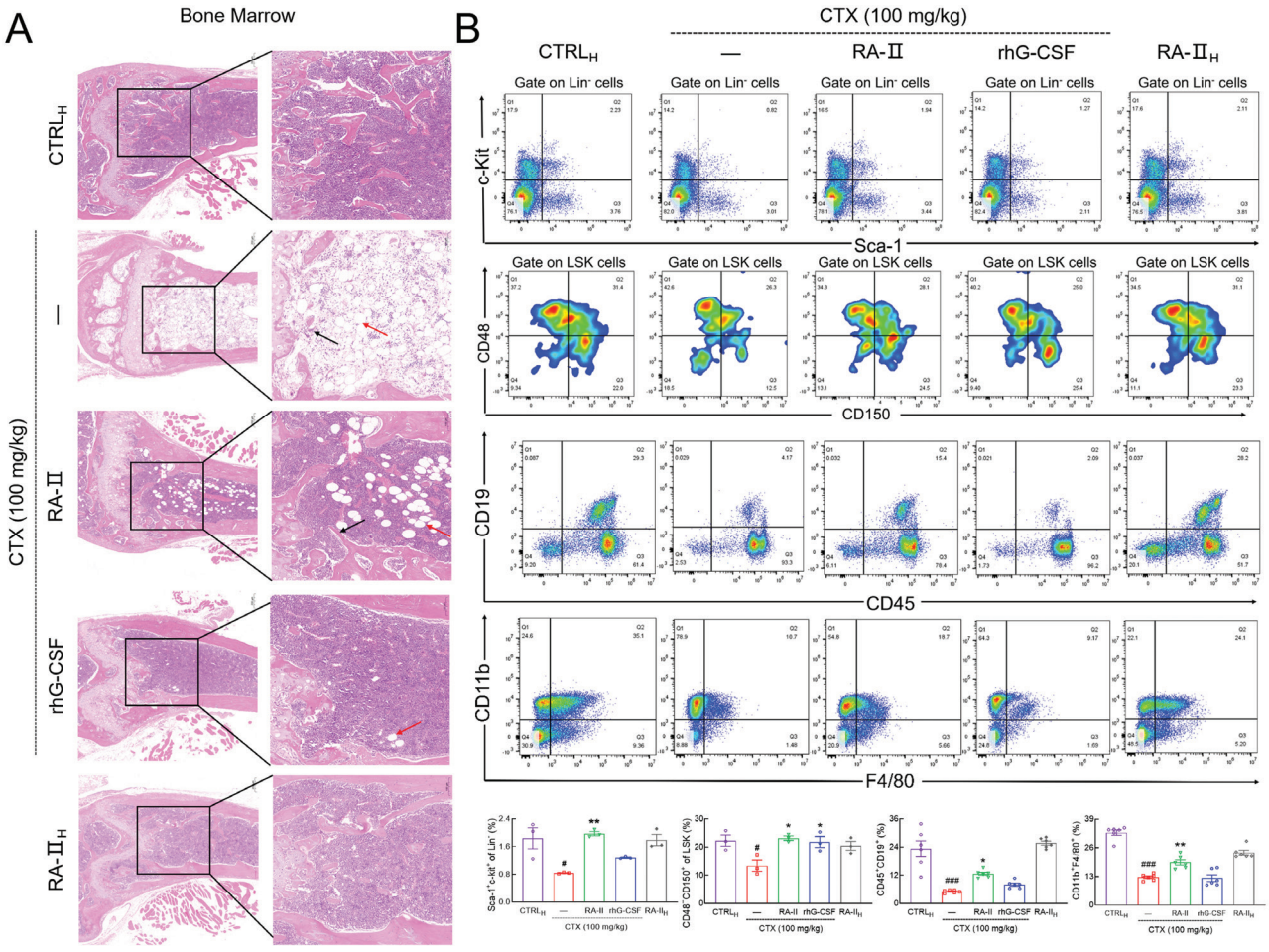

Figure 4 | RA-II alleviates bone marrow injury and elevates hematopoietic cells in mice with hematopoietic dysfunction.
(A) RA-II restored the histomorphology in the bone marrow (100 ×, 200 μm; 200 ×, 100 μm). (B) RA-II enhanced the levels of HSCs (Lin$^-$Sca-1$^+$c-Kit$^+$ [n = 3/group]), LT-HSCs (Lin$^-$Sca-1$^+$c-Kit$^+$CD48$^-$CD150$^+$ [n = 3/group]), B lymphocytes (CD45$^+$CD19$^+$ [n = 6/group]), and macrophages (CD11b$^+$F4/80$^+$ [n = 6/group]) in the bone marrow. Data are presented as the mean ± SEM. $^{\#}P < 0.05$ and $^{\#\#\#}P < 0.001$ *vs.* CTRL$_H$; $^{*}P < 0.05$ and $^{**}P < 0.01$ *vs.* vehicle-treated mice with hematopoietic dysfunction.

promoting macrophage polarization toward the M1 phenotype. RA-II contains high levels of threonine, glycine, and guanine nucleotides; threonine is essential for maintaining primitive HSCs [34]. These substances may serve as the foundation for RA-II to regulate immunity and hematopoiesis.

Bone marrow is the source of myeloid cells, which are crucial for hematopoiesis and immunity in mice [35]. LT-HSCs generate various types of cells necessary for life functions through differentiation and development [35]. NK cells are vital components of the innate immune response [36], while T lymphocytes play an essential role in immune defense [37]. RA-II enhanced splenic NK cell cytotoxic activity, T lymphocyte proliferation, splenic histopathology, and levels of immune factor expression including IgG, IgA, IL-6, and IFN-γ, in immunosuppressed mice. There is a link between immunity and hematopoiesis because hematopoietic and immune cells are derived from HSCs [38]. The immune system safeguards HSCs and supports proper functioning of the hematopoietic system [39]. Excessive suppression of the immune system may negatively affect hematopoiesis [39].

The immune response regulates mobilization and homing of HSCs, and cytokines released by immune cells can influence the quiescence and differentiation of hematopoietic-related cells. Emergence of HSCs is regulated by IL-6 signaling [40]. IL-12 acts synergistically with other cytokines *n vitro* to stimulate the proliferation and differentiation of early hematopoietic progenitor cells [41]. IL-21 maintains homeostasis of hematopoietic progenitor cells [42]. RA-II restored the bone marrow pathology and increased the number of HSCs, LT-HSCs, B lymphocytes, and macrophages in the bone marrow of mice with hematopoietic dysfunction, indicating an improved effect on hematopoiesis.

Acta Materia Medica

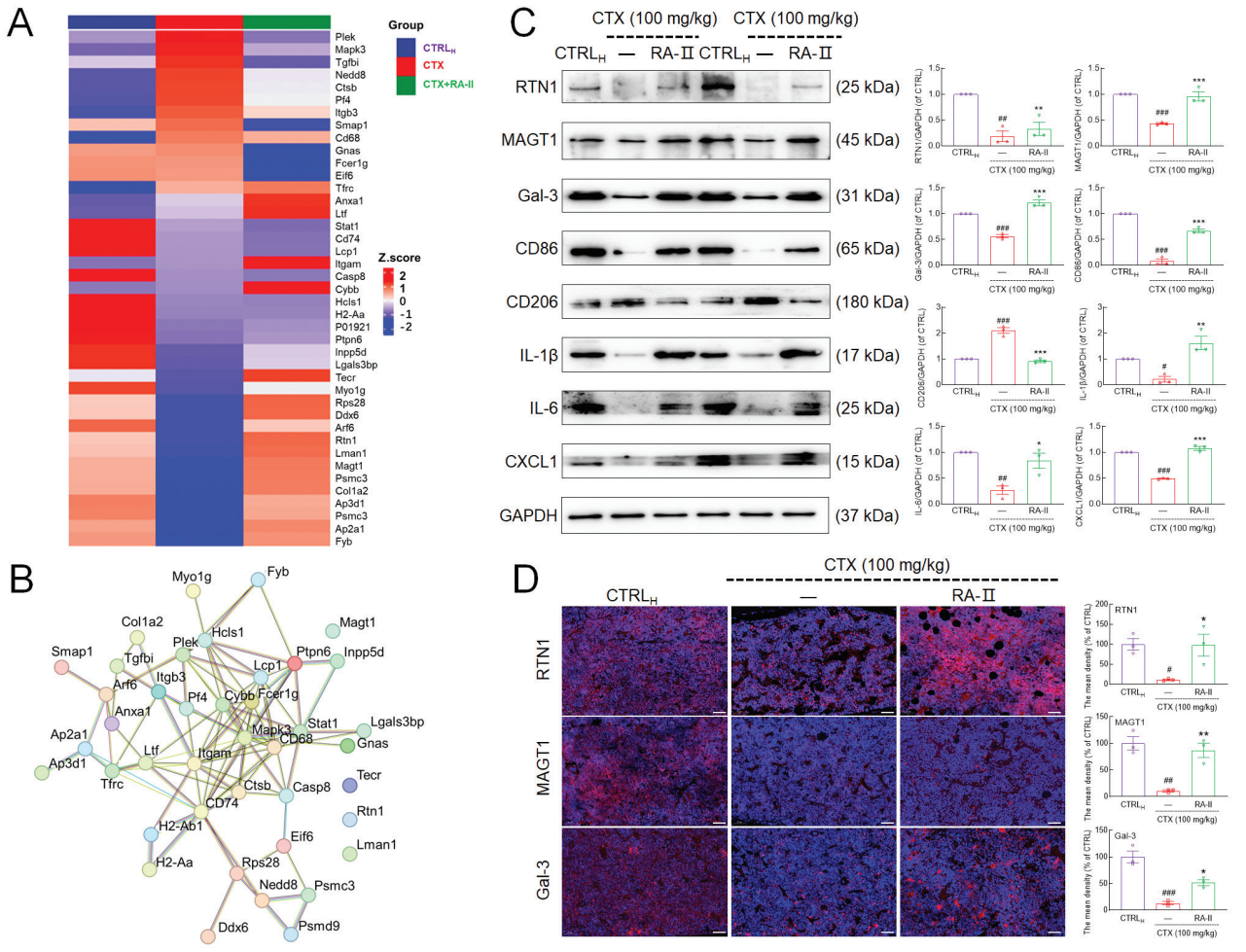

Figure 5 | RA-II regulates macrophages according to proteomic analysis of spleens of mice with hematopoietic dysfunction. (A) Heat map displaying 41 significantly altered proteins. (B) Protein interactions are expected to be analyzed via the STRING database. (C) RA-II enhanced the expression of RTN1, MAGT1, Gal-3, CD86, IL-1β, IL-6, and CXCL1, and suppressed the expression of CD206 in the spleens detected via western blot. (D) RA-II enhanced the expression of RTN1, MAGT1, and Gal-3 in the bone marrow detected via immunohistochemical staining (400 ×, scale bar: 50 μm). Data are presented as the mean ± SEM (n = 3/group). $^{\#}P < 0.05$, $^{\#\#}P < 0.01$, and $^{\#\#\#}P < 0.001$ *vs*. $CTRL_H$; $^{*}P < 0.05$, $^{**}P < 0.01$, and $^{***}P < 0.001$ *vs*. vehicle-treated mice with hematopoietic dysfunction.

The immune response of macrophages is dependent on the gut microbiota, while the regulation of macrophage function is significantly influenced by the gut microbiota [11]. The relative abundance of probiotics, such as *Ruminococcus, Odoribacter*, and *Bacteroides*, was increased in RA-II-treated immunosuppressed mice. *Ruminococcus* and *Odoribacter* have been identified as the primary producers of butyrate, which exerts anti-inflammatory effects through modulation of macrophage function [11, 43]. *Ruminococcus* stimulates the secretion of inflammatory cytokines by macrophages in a TLR4-dependent manner [44] and *Bacteroides* produces bacterial extracellular vesicles that support macrophage survival [45]. The observed alteration of immune responses in the gut microbiota of immunosuppressed mice following administration of RA-II may be attributed to a potential association between RA-II and the gut microbiota.

The association between gut microbiota and serum metabolites has been extensively documented. Following the administration of RA-II, there was a significant increase in the levels of uridine, a serum metabolite that can be converted to uridine diphosphate (UDP). Macrophages express high levels of P2Y6 receptors, which specifically recognize UDP [30]. Addition of uridine also enhances bacterial diversity in mice and facilitates the proliferation of butyrate-producing bacteria, such as unidentified *Ruminococcus* [46]. The positive correlation between uridine and the probiotic, *Ruminococcus*, supports our analysis that RA-II affects macrophage function related to gut microbes and serum metabolites.

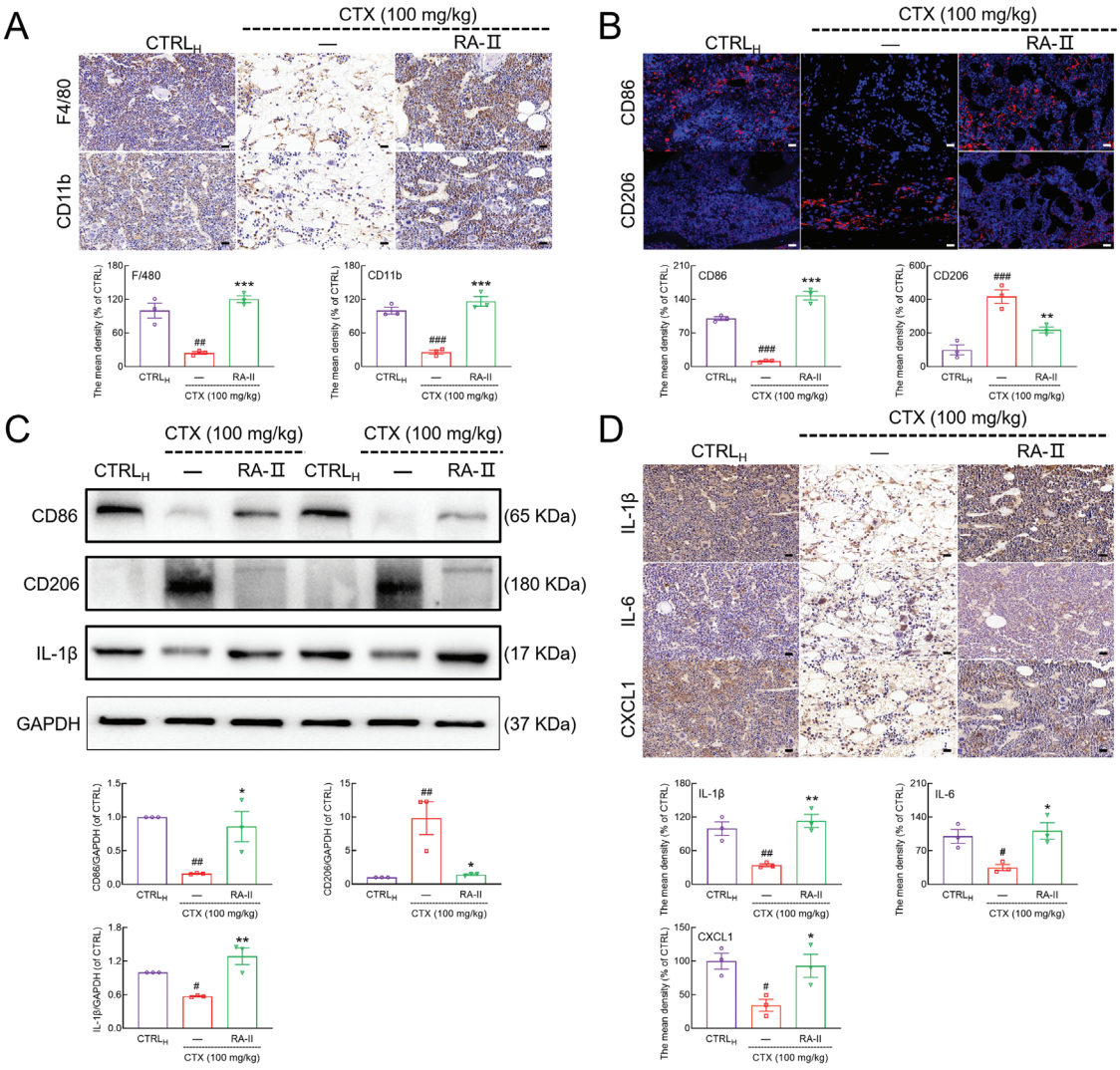

Figure 6 | RA-II promotes macrophage differentiation from M2 towards M1 in mice with hematopoietic dysfunction.
(A) RA-II enhanced the expression of F4/80 and CD11b in the bone marrow detected via immunohistochemical staining (400 ×, scale bar: 20 μm). (B) RA-II enhanced the expression of CD86 and suppressed the expression of CD206 in the bone marrow detected using immunofluorescence (400 ×, scale bar: 20 μm). (C) RA-II enhanced the expression of CD86 and IL-1β, and suppressed the expression of CD206 in the bone marrow detected via western blot. (D) RA-II enhanced the expression of IL-1β, IL-6, and CXCL1 in the bone marrow analyzed via immunohistochemical staining (400 ×, scale bar: 20 μm). Data are presented as the mean ± SEM (n = 3/group). $^{\#}P < 0.05$, $^{\#\#}P < 0.01$, and $^{\#\#\#}P < 0.001$ *vs.* $CTRL_H$; $^{*}P < 0.05$, $^{**}P < 0.01$, and $^{***}P < 0.001$ *vs.* vehicle-treated mice with hematopoietic dysfunction.

Furthermore, administration of RA-II significantly decreased the serum levels of 12(S)-HETE and L-carnitine, while concurrently increasing serum levels of solasodine, all of which are associated with macrophages. The presence of 12(S)-HETE inhibits macrophage phagocytosis of apoptotic cells and suppresses IL-10 secretion [47]. Direct inhibition of macrophage activation and cytokine production, including IL-6, IL-1β, and TNF-α, has been observed with L-carnitine. Additionally, 12(S)-HETE may hinder polarization of macrophages towards the M2 phenotype by inducing trimethylamine N-oxide (TMAO) production [31, 48]. Imbalanced macrophage polarization towards M1 or M2 impairs immune response efficiency [3]. RA-II may influence macrophage differentiation, especially polarization of M1 phenotype, during immune promotion.

Macrophages differentiate from monocytes developing from HSCs in the bone marrow [49]. The significant influence of RA-II on proteins has been shown to correlate with regulation of the immune system, hematopoiesis, and myeloid cell differentiation. Involvement of RTN1 in hematopoietic cell formation is associated with a potential upregulation of M1 macrophages due to high expression [50]. MAGT1 enhances the proliferation

of hematopoietic stem cells and lymphocytes [51]. Lgals3bp upregulates Gal-3 levels, acting as a negative regulator of the cell cycle in HSCs [52, 53]. Gal-3 also stimulates M1 macrophages to secrete IL-1β [54].

Accordingly, iNOS and CD86 are recognized as markers of M1 macrophages, while ARG1 and CD206 are recognized as markers of M2 macrophages [55]. M1 macrophages influence the levels of pro-inflammatory cytokines [55-57]. RA-II elevated the number of macrophages, increased CD86 expression, and decreased CD206 expression in the bone marrow, confirming promotion of macrophage differentiation from M2 towards M1 in hematopoietic dysfunction mice. Stimulation of M1 macrophages leads to an increase in the level of cytokine secretion, such as IL-1β, IL-6, and CXCL1 [58, 59]. IL-1β significantly enhances hematopoiesis. IL-1R1 serves as the primary receptor for transducing IL-1 signaling in hematopoietic cells. IL-1R1 is expressed in various subpopulations of hematopoietic stem and progenitor cells (HSPCs), including LT-HSCs. Through its interaction with IL-1R1, IL-1β directly impacts HSPCs [60]. The direct action of IL-1β on HSPCs promotes proliferation and differentiation, while simultaneously inhibiting apoptosis [60] and enhancing hematopoietic support [61]. In addition, signaling of IL-1β improves radiation-induced HSPC death. Impaired IL-1β/IL-1R1 signaling may hinder hematopoietic regeneration following radiotherapy and transplantation. In conclusion, IL-1β has a significant role in protecting blood cells against radiation damage and has the potential to enhance hematopoietic regeneration after radiotherapy [60]. The increased production of IL-1β enhances the expression of CXCL1, which has a crucial role in maintaining the self-renewal capacity of HSCs [62]. CXCL1 interacts with CXCR2 ligands expressed on relevant hematopoietic cells and is essential for hematopoiesis [62]. Additionally, the role of CXCL1 in the regulation of hematopoiesis within the bone marrow niche is crucial because CXCL1 effectively modulates the quiescent HSC pool [63, 64]. IL-6 activates gp130 signaling through binding to the IL-6R receptor, thereby promoting the proliferation and maturation of HSPCs [65]. Specifically, IL-6 primarily promotes HSPC proliferation and myeloid differentiation along the monocyte lineage [66]. Our data demonstrated that RA-II has a role in enhancing hematopoiesis by promoting macrophage polarization towards the M1 phenotype and releasing related regulatory factors, such as IL-1β, IL-6, and CXCL1.

There were some limitations to this study. Although we demonstrated the hematopoietic-promoting effect of RA-II in animal studies, further confirmation through clinical trials is necessary to establish its potential as a therapeutic agent for enhancing hematopoiesis in patients. Furthermore, although we observed changes in the gut microbiome of immunosuppressed mice after the administration of RA-II, it remains unclear whether RA-II directly or indirectly influence these alterations. We plan to conduct corollary studies involving microbiota reconstitution in mice depleted of gut microbiota to clarify this finding. Our subsequent investigations will aim to further elucidate the pure active constituents within RA-II to identify specific target molecules and unravel the associated signaling pathways. Other significantly altered proteins identified through proteomics analysis and the regulation of these proteins in hematopoiesis warrant verification.

5. CONCLUSIONS

This study represents the pioneering evidence confirming the immune-boosting and hematopoietic-promoting effects of RA-II using immunosuppressed and hematopoietic dysfunction murine models based on material studies. Combined with multi-omics analysis and validation, RA-II function may be associated with the release of immune- and hematopoietic-related factors induced by macrophage stimulation after differentiation to M1. Our study provides a theoretical basis for application of RA-II on hematopoietic dysfunction in the clinical setting.

ACKNOWLEDGMENTS

This work was supported by the Science and Technology Development Project of Jilin Province-Construction of Regional Innovation Systems (No. YDZJ202404003QYCX), and the Science Fund for Distinguished Young Scholars of Jilin Province, China (No. 20230101356JC).

CONFLICT OF INTEREST

The authors declare no conflicts of interest.

ETHICS APPROVAL AND CONSENT TO PARTICIPATE

The experiments complied with the ARRIVE guidelines and were carried out in accordance with the National Institutes of Health Guide for the Care and Use of Laboratory Animals. Additionally, an ethical review form regarding animal welfare was obtained and approved by the Institution Animal Ethics Committee of Jilin University (Nos. SY202207013 and SY202207014). All participants have been informed of the potential risks and benefits of the study and have signed an informed consent form.

CONSENT FOR PUBLICATION

Not applicable.

DATA AVAILABILITY

All data generated or analyzed is included in the published article and its supplementary information files.

REFERENCES

[1] Chen S, Saeed A, Liu Q, Jiang Q, Xu H, Xiao GG, et al.: Macrophages in Immunoregulation and Therapeutics. *Signal Transduction and Targeted Therapy* 2023, 8:207.

[2] Liang G, Zhou C, Jiang X, Zhang Y, Huang B, Gao S, et al.: De Novo Generation of Macrophage from Placenta-Derived Hemogenic Endothelium. *Developmental Cell* 2021, 56:2121–2133.
[3] Herrada AA, Olate-Briones A, Lazo-Amador R, Liu C, Hernández-Rojas B, Riadi G, et al.: Lymph Leakage Promotes Immunosuppression by Enhancing Anti-Inflammatory Macrophage Polarization. *Frontiers in Immunology* 2022, 13:841641.
[4] Oyarce C, Vizcaino-Castro A, Chen S, Boerma A, Daemen T: Re-Polarization of Immunosuppressive Macrophages to Tumor-Cytotoxic Macrophages by Repurposed Metabolic Drugs. *OncoImmunology* 2021, 10:1898753.
[5] Gu J, Chu X, Huo Y, Liu C, Chen Q, Hu S, et al.: Gastric Cancer-Derived Exosomes Facilitate Pulmonary Metastasis by Activating ERK-Mediated Immunosuppressive Macrophage Polarization. *Journal of Cellular Biochemistry* 2023, 124:557-572.
[6] Hao S, Wang Y, Dong F, Cheng T: Crosstalk between Hematopoietic Stem Cells and Immune System. *Zhonghua Xue Ye Xue Za Zhi* 2015, 36:1043-1048.
[7] Takizawa H. Innate Immune Signal-Regulated Hematopoiesis. *Blood* 2019, 134:SCI-1.
[8] Vallelonga V, Gandolfi F, Ficara F, Della Porta MG, Ghisletti S: Emerging Insights into Molecular Mechanisms of Inflammation in Myelodysplastic Syndromes. *Biomedicines* 2023, 11:2613.
[9] Kim D, Zeng MY, Núñez G: The Interplay between Host Immune Cells and Gut Microbiota in Chronic Inflammatory Diseases. *Experimental & Molecular Medicine* 2017, 49:e339.
[10] Zhang Y, Gao X, Gao S, Liu Y, Wang W, Feng Y, et al.: Effect of Gut Flora Mediated-Bile Acid Metabolism on Intestinal Immune Microenvironment. *Immunology* 2023, 170:301-318.
[11] Wang J, Chen W-D, Wang Y-D: The Relationship between Gut Microbiota and Inflammatory Diseases: The Role of Macrophages. *Frontiers in Microbiology* 2020, 11:1065.
[12] Hua H, Pan C, Chen X, Jing M, Xie J, Gao Y, et al.: Probiotic Lactic Acid Bacteria Alleviate Pediatric IBD and Remodel Gut Microbiota by Modulating Macrophage Polarization and Suppressing Epithelial Apoptosis. *Frontiers in Microbiology* 2023, 14:1168924.
[13] Zhu Z, Yi B, Tang Z, Chen X, Li M, Xu T, et al.: Lactobacillus Casei Combined with Lactobacillus Reuteri Alleviate Pancreatic Cancer by Inhibiting TLR4 to Promote Macrophage M1 Polarization and Regulate Gut Microbial Homeostasis. *BMC Cancer* 2023, 23:1044.
[14] MacNamara KC, Nolte MA: Code Red in the Supply Center: The Impact of Immune Activation on Hematopoiesis. *Cells* 2022, 11:1586.
[15] Mariani SA, Li Z, Rice S, Krieg C, Fragkogianni S, Robinson M, et al.: Pro-Inflammatory Aorta-Associated Macrophages are Involved in Embryonic Development of Hematopoietic Stem Cells. *Immunity* 2019, 50:1439-1452.
[16] Zhang T, Zhou M, Xiao D, Liu Z, Jiang Y, Feng M, et al.: Myelosuppression Alleviation and Hematopoietic Regeneration by Tetrahedral-Framework Nucleic-Acid Nanostructures Functionalized with Osteogenic Growth Peptide. *Advanced Science* 2022, 9:e2202058.
[17] Ustyuzhanina NE, Anisimova NY, Bilan MI, Donenko FV, Morozevich GE, Yashunskiy DV, et al.: Chondroitin Sulfate and Fucosylated Chondroitin Sulfate as Stimulators of Hematopoiesis in Cyclophosphamide-Induced Mice. *Pharmaceuticals* 2021, 14:1074.
[18] Hou T, Wang T, Mu W, Yang R, Liang S, Zhang Z, et al.: Nanoparticle-Loaded Polarized-Macrophages for Enhanced Tumor Targeting and Cell-Chemotherapy. *Nano-Micro Letters* 2020, 13:6.
[19] Li M-Z, Huang X-J, Hu J-L, Cui SW, Xie M-Y, Nie S-P: The Protective Effects against Cyclophosphamide (CTX)-Induced Immunosuppression of Three Glucomannans. *Food Hydrocolloids* 2020, 100:105445.
[20] Li L, Jiang X, Teng S, Zhang L, Teng L, Wang D: Calf Thymus Polypeptide Improved Hematopoiesis via Regulating Colony-Stimulating Factors in BALB/c Mice with Hematopoietic Dysfunction. *International Journal of Biological Macromolecules* 2020, 156:204-216.
[21] Zheng W, Xu D, Wang M, Zhang Y, Gao Q, Gao Y: Fingerprint Analysis and Multi-Component Determination of Ribonucleic Acid for Injection II Recipe by HPLC–DAD and LC–ESI-MS Methods. *Journal of Chromatographic Science* 2018, 57:238-242.
[22] Zhao F, Qian J, Liu H, Wang C, Wang X, Wu W, et al.: Quantification, Identification and Comparison of Oligopeptides on Five Tea Categories with Different Fermentation Degree by Kjeldahl Method and Ultra-High Performance Liquid Chromatography Coupled with Quadrupole-Orbitrap Ultra-High Resolution Mass Spectrometry. *Food Chemistry* 2022, 378:132130.
[23] Wang S, Zhang Y, Meng W, Dong Y, Zhang S, Teng L, et al.: The Involvement of Macrophage Colony Stimulating Factor on Protein Hydrolysate Injection Mediated Hematopoietic Function Improvement. *Cells* 2021, 10:2776.
[24] Li S, Yang H, Li L, Wang W, Tan HY, Qu Y, et al.: The Involvement of Gut Microbiota in the Anti-Tumor Effect of Carnosic Acid via IL-17 Suppression in Colorectal Cancer. *Chemico-Biological Interactions* 2022, 365:110080.
[25] Dong M, Liu H, Cao T, Li L, Sun Z, Qiu Y, et al.: Huoxiang Zhengqi Alleviates Azoxymethane/Dextran Sulfate Sodium-Induced Colitis-Associated Cancer by Regulating Nrf2/NF-κB/NLRP3 Signaling. *Frontiers in Pharmacology* 2022, 13:1002269.
[26] Wang Y, Viollet B, Terkeltaub R, Liu-Bryan R: AMP-Activated Protein Kinase Suppresses Urate Crystal-Induced Inflammation and Transduces Colchicine Effects in Macrophages. *Annals of the Rheumatic Diseases* 2016, 75:286-294.
[27] Wen Y, Gu J, Chakrabarti SK, Aylor K, Marshall J, Takahashi Y, et al.: The Role of 12/15-Lipoxygenase in the Expression of Interleukin-6 and Tumor Necrosis Factor-alpha in Macrophages. *Endocrinology* 2007, 148:1313-1322.
[28] Korbecki J, Bajdak-Rusinek K: The Effect of Palmitic Acid on Inflammatory Response in Macrophages: An Overview of Molecular Mechanisms. *Inflammation Research* 2019, 68:915-932.
[29] Chiu FL, Lin JK: Tomatidine Inhibits iNOS and COX-2 through Suppression of NF-kappaB and JNK Pathways in LPS-Stimulated Mouse Macrophages. *FEBS Letters* 2008, 582:2407-2412.
[30] Nagai J, Lin J, Boyce JA: Macrophage P2Y6 Receptor Signaling Selectively Activates NFATC2 and Suppresses Allergic Lung Inflammation. *Journal of Immunology* 2022, 209:2293-2303.
[31] Fortin G, Yurchenko K, Collette C, Rubio M, Villani AC, Bitton A, et al.: L-Carnitine, a Diet Component and Organic Cation Transporter OCTN Ligand, Displays Immunosuppressive Properties and Abrogates Intestinal

Inflammation. *Clinical and Experimental Immunology* 2009, 156:161-171.

[32] Kang Z-P, Wang M-X, Wu T-T, Liu DY, Wang HY, Long J, et al.: Curcumin Alleviated Dextran Sulfate Sodium-Induced Colitis by Regulating M1/M2 Macrophage Polarization and TLRs Signaling Pathway. *Evidence-Based Complementary and Alternative Medicine* 2021, 2021:3334994.

[33] Peng K, Deng N, Meng Y, He Q, Meng H, Luo T, et al.: Alpha-Momorcharin Inhibits Proinflammatory Cytokine Expression by M1 Macrophages but not Anti-Inflammatory Cytokine Expression by M2 Macrophages. *Journal of Inflammation Research* 2022, 15:4853-4872.

[34] Li Z, Takubo K, Qian P, Suda T, Li L: Amino Acid Transporter X is Required for Hematopoietic Stem Cell Maintenance through Regulating Specific Amino Acids Level. *Blood* 2015, 126:1166-1166.

[35] Sureshchandra S, Chan CN, Robino JJ, Parmelee LK, Nash MJ, Wesolowski SR, et al.: Maternal Western-Style Diet Remodels the Transcriptional Landscape of Fetal Hematopoietic Stem and Progenitor Cells in Rhesus Macaques. *Stem Cell Reports* 2022, 17:2595-2609.

[36] Shi Y, Pan J, Hang C, Tan L, Hu L, Yan Z, et al.: The Estrogen/miR-338-3p/ADAM17 Axis Enhances the Viability of Breast Cancer Cells via Suppressing NK Cell's Function. *Environmental Toxicology* 2023, 38:1618-1627.

[37] Yang J, Lv Y, Zhu Y, Li S, Tao J, Chang L, et al.: Baseline T-Lymphocyte and Cytokine Indices in Sheep Peripheral Blood. *BMC Veterinary Research* 2022, 18:165.

[38] Filippi M-D: Hematopoietic Stem Cell (HSC) Divisional Memory: The Journey of Mitochondrial Metabolism through HSC Division. *Experimental Hematology* 2021, 96:27-34.

[39] Huang J, Pu Y, Xu K, Ding Q, Sun R, Yin L, et al.: High Expression of HIF-1α Alleviates Benzene-Induced Hematopoietic Toxicity and Immunosuppression in Mice. *Environmental Pollution* 2022, 311:119928.

[40] Tie R, Li H, Cai S, Liang Z, Shan W, Wang B, et al.: Interleukin-6 Signaling Regulates Hematopoietic Stem Cell Emergence. *Experimental & Molecular Medicine* 2019, 51:1-12.

[41] Eng VM, Car BD, Schnyder B, Lorenz M, Lugli S, Aguet M, et al.: The Stimulatory Effects of Interleukin (IL)-12 on Hematopoiesis are Antagonized by IL-12-Induced Interferon Gamma in Vivo. *Journal of Experimental Medicine* 1995, 181:1893-1898.

[42] Kaplan MH, Glosson NL, Stritesky GL, Yeh N, Kinzfogl J, Rohrabaugh SL, et al.: STAT3-Dependent IL-21 Production from T Helper Cells Regulates Hematopoietic Progenitor Cell Homeostasis. *Blood* 2011, 117:6198-6201.

[43] Wang R, Lin F, Ye C, Aihemaitijiang S, Halimulati M, Huang X, et al.: Multi-Omics Analysis Reveals Therapeutic Effects of Bacillus Subtilis-Fermented Astragalus Membranaceus in Hyperuricemia via Modulation of Gut Microbiota. *Food Chemistry* 2023, 399:133993.

[44] Henke MT, Kenny DJ, Cassilly CD, Vlamakis H, Xavier RJ, Clardy J: Ruminococcus Gnavus, a Member of the Human Gut Microbiome Associated with Crohn's Disease, Produces an Inflammatory Polysaccharide. *Proceedings of the National Academy of Sciences of the United States of America* 2019, 116:12672-12677.

[45] Gul L, Modos D, Fonseca S, Madgwick M, Thomas JP, Sudhakar P, et al.: Extracellular Vesicles Produced by the Human Commensal Gut Bacterium Bacteroides Thetaiotaomicron Affect Host Immune Pathways in a Cell-Type Specific Manner that are Altered in Inflammatory Bowel Disease. *Journal of Extracellular Vesicles* 2022, 11:e12189.

[46] Liu Y, Xie C, Zhai Z, Deng ZY, De Jonge HR, Wu X, et al.: Uridine Attenuates Obesity, Ameliorates Hepatic Lipid Accumulation and Modifies the Gut Microbiota Composition in Mice Fed with a High-Fat Diet. *Food & Function* 2021, 12:1829-1840.

[47] Manega CM, Fiorelli S, Porro B, Turnu L, Cavalca V, Bonomi A, et al.: 12(S)-Hydroxyeicosatetraenoic Acid Downregulates Monocyte-Derived Macrophage Efferocytosis: New Insights in Atherosclerosis. *Pharmacological Research* 2019, 144:336-342.

[48] Shi W, Huang Y, Yang Z, Zhu L, Yu B: Reduction of TMAO Level Enhances the Stability of Carotid Atherosclerotic Plaque through Promoting Macrophage M2 Polarization and Efferocytosis. *Bioscience Reports* 2021, 41:BSR20204250.

[49] Ju W, Sun T, Lu W, Xu K, Qiao J, Zeng L: The Role of Macrophages in Bone Marrow Injury and Hematopoietic Reconstitution. *Blood* 2019, 134:3729-3729.

[50] Zhu S, Zu L, Xu S: The Expression of RTN1 in Lung Adenocarcinoma and its Effect on Immune Microenvironment. *Zhongguo Fei Ai Za Zhi* 2022, 25:385-395.

[51] Brault J, Liu T, Bello E, Liu S, Sweeney CL, Meis RJ, et al.: CRISPR-Targeted MAGT1 Insertion Restores XMEN Patient Hematopoietic Stem Cells and Lymphocytes. *Blood* 2021, 138:2768-2780.

[52] Li J, Zhao C, Li Y, Wen J, Wang S, Wang D, et al.: Osteosarcoma Exocytosis of Soluble LGALS3BP Mediates Macrophages Toward a Tumoricidal Phenotype. *Cancer Letters* 2022, 528:1-15.

[53] Chen Y, Wang H, Shen J, Deng R, Yao X, Guo Q, et al.: Gasdermin D Drives the Nonexosomal Secretion of Galectin-3, an Insulin Signal Antagonist. *Journal of Immunology* 2019, 203:2712-2723.

[54] Uchino Y, Woodward AM, Mauris J, Peterson K, Verma P, Nilsson UJ, et al.: Galectin-3 is an Amplifier of the Interleukin-1β-Mediated Inflammatory Response in Corneal Keratinocytes. *Immunology* 2018, 154:490-499.

[55] Yan S, Zhou M, Zheng X, Xing Y, Dong J, Yan M, et al.: Anti-Inflammatory Effect of Curcumin on the Mouse Model of Myocardial Infarction through Regulating Macrophage Polarization. *Mediators of Inflammation* 2021, 2021:9976912.

[56] Liu P, Liu X, Zhang L, Yan G, Zhang H, Xu D, et al.: ALA-PDT Augments Intense Inflammation in the Treatment of Acne Vulgaris by COX2/TREM1 Mediated M1 Macrophage Polarization. *Biochemical Pharmacology* 2023, 208:115403.

[57] Xu X, Wang X, Guo Y, Bai Y, He S, Wang N, et al.: Inhibition of PTP1B Promotes M2 Polarization via microRNA-26a/MKP1 Signaling Pathway in Murine Macrophages. *Frontiers in Immunology* 2019, 10:1930.

[58] Barsheshet Y, Brant B, Voloshin T, Volodin A, Koren L, Klein-Goldberg A, et al.: 726 Tumor Treating Fields (TTFields) Induce an Altered Polarization Program in M1/M2 Macrophages. *Journal for ImmunoTherapy of Cancer* 2021, 9:A756.

[59] Di Vincenzo S, Ferraro M, Taverna S, Malizia V, Buscetta M, Cipollina C, et al.: Tyndallized Bacteria Preferentially Induce Human Macrophage M1 Polarization: An Effect Useful to Balance Allergic Immune Responses and to Control Infections. *Antibiotics* 2023, 12:571.

[60] Guo R, Zhang X, Liu P, Ren Q, Xie X, Gao R, et al.: Heat-Inactivated Escherichia coli Promotes Hematopoietic Regeneration after Irradiation with IL-1β. *Cytotherapy* 2022, 24:172-182.
[61] Ji YR, Yang ZX, Li LN, Han ZB, Chi Y, Han ZC: IL-1β Promotes the Hematopoietic Support of Human Umbilical Cord Mesenchymal Stem Cells. *Zhongguo Shi Yan Xue Ye Xue Za Zhi* 2013, 21:1005-1009.
[62] Korbecki J, Gąssowska-Dobrowolska M, Wójcik J, Szatkowska I, Barczak K, Chlubek M, et al.: The Importance of CXCL1 in Physiology and Noncancerous Diseases of Bone, Bone Marrow, Muscle and the Nervous System. *International Journal of Molecular Sciences*. 2022;23:4205.
[63] Zhang P, Chen Z, Li R, Guo Y, Shi H, Bai J, et al.: Loss of ASXL1 in the Bone Marrow Niche Dysregulates Hematopoietic Stem and Progenitor Cell Fates. *Cell Discovery* 2018, 4:4.
[64] Sinclair A, Park L, Shah M, Drotar M, Calaminus S, Hopcroft LE, et al.: CXCR2 and CXCL4 Regulate Survival and Self-Renewal of Hematopoietic Stem/Progenitor Cells. *Blood* 2016, 128:371-383.
[65] Kimura T, Wang J, Minamiguchi H, Fujiki H, Harada S, Okuda K, et al.: Signal through gp130 Activated by Soluble Interleukin (IL)-6 Receptor (R) and IL-6 or IL-6R/IL-6 Fusion Protein Enhances ex vivo Expansion of Human Peripheral Blood-Derived Hematopoietic Progenitors. *Stem Cells* 2000, 18:444-452.
[66] Boettcher S, Manz MG: Regulation of Inflammation- and Infection-Driven Hematopoiesis. *Trends in Immunology* 2017, 38:345-357.